Observations and simulations of formation of broad plasma depletions through merging process

Chao-Song Huang,[1] J. M. Retterer,[2] O. de La Beaujardiere,[1] P. A. Roddy,[1] D. E. Hunton,[1] J. O. Ballenthin,[1] and R. F. Pfaff[3]

Received 18 August 2011; revised 29 November 2011; accepted 16 December 2011; published 23 February 2012.

[1] Broad plasma depletions in the equatorial ionosphere near dawn are region in which the plasma density is reduced by 1–3 orders of magnitude over thousands of kilometers in longitude. This phenomenon is observed repeatedly by the Communication/Navigation Outage Forecasting System (C/NOFS) satellite during deep solar minimum. The plasma flow inside the depletion region can be strongly upward. The possible causal mechanism for the formation of broad plasma depletions is that the broad depletions result from merging of multiple equatorial plasma bubbles. The purpose of this study is to demonstrate the feasibility of the merging mechanism with new observations and simulations. We present C/NOFS observations for two cases. A series of plasma bubbles is first detected by C/NOFS over a longitudinal range of 3300–3800 km around midnight. Each of the individual bubbles has a typical width of ~100 km in longitude, and the upward ion drift velocity inside the bubbles is 200–400 m s^{-1}. The plasma bubbles rotate with the Earth to the dawn sector and become broad plasma depletions. The observations clearly show the evolution from multiple plasma bubbles to broad depletions. Large upward plasma flow occurs inside the depletion region over 3800 km in longitude and exists for ~5 h. We also present the numerical simulations of bubble merging with the physics-based low-latitude ionospheric model. It is found that two separate plasma bubbles join together and form a single, wider bubble. The simulations show that the merging process of plasma bubbles can indeed occur in incompressible ionospheric plasma. The simulation results support the merging mechanism for the formation of broad plasma depletions.

Citation: Huang, C.-S., J. M. Retterer, O. de La Beaujardiere, P. A. Roddy, D. E. Hunton, J. O. Ballenthin, and R. F. Pfaff (2012), Observations and simulations of formation of broad plasma depletions through merging process, *J. Geophys. Res.*, *117*, A02314, doi:10.1029/2011JA017084.

1. Introduction

[2] Broad plasma depletions detected by the Communication/Navigation Outage Forecasting System (C/NOFS) satellite near dawn are significant decreases of plasma density in the low-latitude ionosphere over a very large longitudinal range (1000–4000 km) [*Burke et al.*, 2009; *de La Beaujardière et al.*, 2009; *Huang et al.*, 2009; *Kelley et al.*, 2009; *Su et al.*, 2009; *Huang et al.*, 2011]. Different mechanisms have been proposed to explain the generation of the broad region of reduced plasma density. *Huang et al.* [2009] suggested that the formation of broad plasma decreases could be related to a cooling or downwelling of the ionosphere and thermosphere in the equatorial region and ruled out the possibility of plasma bubbles as the cause of broad plasma decreases. The ion vertical velocity is small or weakly downward in the ionospheric downwelling process.

[3] *Huang et al.* [2011] reported the observations that upward plasma drift of 200–300 m s^{-1} occurs in the broad depletion region. The new type of broad plasma depletions is different from those caused by ionospheric downwelling [*Huang et al.*, 2009] in two aspects. The first major difference is the presence of large upward plasma drift, and the second is the role of equatorial plasma bubbles in the formation of broad plasma depletions. *Huang et al.* [2011] proposed the following mechanism for the generation of the new type of broad plasma depletions. A series of equatorial plasma bubbles starts to form in the bottomside *F* region over a broad longitude range in the evening sector. Each of the bubbles is produced by the Rayleigh-Taylor instability process, and the upward ion drift is related to the polarization electric field inside the bubbles. During the growing and rising process, the longitudinal width of the bubbles increases, and two or more bubbles merge to form a wider bubble or broad plasma depletions. The upward ion drift velocity inside individual bubbles remains large after the bubbles have

[1]Space Vehicles Directorate, Air Force Research Laboratory, Kirtland AFB, New Mexico, USA.
[2]Institute for Scientific Research, Boston College, Chestnut Hill, Massachusetts, USA.
[3]Space Weather Laboratory, NASA Goddard Space Flight Center, Greenbelt, Maryland, USA.

This paper is not subject to U.S. copyright.
Published in 2012 by the American Geophysical Union.

merged to form broad depletions. An important property of the mechanism is that the broad plasma depletions result from merging of multiple plasma bubbles.

[4] The physical process for the generation of plasma bubbles in the equatorial ionosphere has been well understood. Plasma bubbles are generated through nonlinear evolution of the Rayleigh-Taylor instability [*Haerendel*, 1973; *Woodman and La Hoz*, 1976; *Scannapieco and Ossakow*, 1976; *Zalesak et al.*, 1982; *Tsunoda and White*, 1981; *Kelley et al.*, 1986; *Huang and Kelley*, 1996a, 1996b; *Keskinen et al.*, 2003; *Huba et al.*, 2009; *Krall et al.*, 2010; *Retterer*, 2010a, 2010b]. The Rayleigh-Taylor instability is excited in the bottomside *F* region and evolves into a plasma bubble that penetrates the *F* peak to the topside *F* region. The typical width of a fully developed plasma bubble is ~100 km in longitude. A plasma bubble is also termed as plasma depletion when the decrease of plasma density is addressed in the literature.

[5] It is necessary to briefly discuss the terminology of large-scale reduction in plasma density detected by C/NOFS. *Huang et al.* [2009] used "broad plasma deceases" to describe the plasma decreases associated with downwelling of the thermosphere, and the ion vertical velocity is small or weakly downward. *Burke et al.* [2009] used "plasma trenches" to describe the longitudinally broad region with reduced plasma density. *Su et al.* [2009, 2011] used the physics-based ionospheric model (PBMOD) to reproduce "large-scale depletions" in plasma density. *Huang et al.* [2011] analyzed the formation and evolution of reduced plasma regions with multiple plasma bubbles over a large longitudinal range. They found that the reduced plasma regions are not generated in the dawn sector. Instead, multiple plasma bubbles originate in the evening sector, rotate with the Earth to the post-midnight sector, and finally evolve into large-scale depletions near dawn. The ion density and velocity are highly structured in the midnight sector because of the existence of plasma bubbles. In order to distinguish the difference between equatorial plasma bubbles and broad depletion regions, *Huang et al.* [2011] use "plasma bubble" to describe the plasma density decrease over a relatively small range (~100 km in longitude, the typical width of a fully developed bubble), "wide bubble" to describe the plasma density decrease over several hundreds of kilometers in longitude, and "broad plasma depletion" to describe the plasma density decrease over a very large longitudinal range (e.g., greater than 1000 km). The term "broad plasma depletion" is used for the depletion region with multiple plasma bubbles. A broad plasma depletion is not a single large bubble, and multiple bubbles exist inside the broad depletion region. In the present study, we use the same terminology as that defined by *Huang et al.* [2011].

[6] In the mechanism proposed by *Huang et al.* [2011], the merging process of multiple plasma bubbles is the key factor for the formation of broad plasma depletions. When two or more plasma bubbles are present, the plasma density is greatly reduced inside each bubble but remains nearly the same as the background density in the region between successive bubbles. The plasma flow is upward inside individual bubbles and weakly downward in the region between different bubbles. If two bubbles merge to form a single wider bubble, the downward-moving, high-density region between the bubbles must disappear. However, the ionospheric plasma is nearly incompressible. The critical issues are how the high density barriers between different bubbles can be removed and whether the merging process can indeed occur in incompressible plasma. In this study, we present C/NOFS measurements of broad plasma depletions and numerical simulations of merging of plasma bubbles. The purpose of this study is to show the occurrence of broad plasma depletions with strong upward plasma flow over 3800 km in longitude and to justify the feasibility of the merging process.

2. Observations

[7] We first present measurements of ion density and ion vertical velocity with the C/NOFS satellite on 9–10 June 2008. Figure 1a shows the latitude and altitude of C/NOFS, Figure 1b shows the ion density, and Figure 1c shows the ion vertical velocity. The ion density and ion velocity during each orbit are plotted in the same row. For each orbit, the orbit number is given in Figure 1a, and the UT is given in Figure 1b. All data are plotted as a function of solar local time at the satellite position. The shift of continents from one orbit to next corresponds to the rotation of the Earth. The ion vertical velocity in Figure 1c is calculated from the electric field measured by the Vector Electric Field Instrument (VEFI) on board C/NOFS [*Pfaff et al.*, 2010]. We have converted the electric field into ion drift velocity to show the plasma motion.

[8] The yellow shading in Figure 1 shows where the broad plasma depletion is forming. In the depletion region, the orbit of C/NOFS is close to the magnetic equator, and the altitude of C/NOFS is 400–500 km. During Orbit 803 (top row), perturbations in the ion density are relatively small, except for the one near the eastern boundary of the shaded region, and the ion vertical velocity is slightly enhanced over the background plasmas drift. Because the plasma density decreases and velocity enhancements become much larger at later times, the variations of the ion density and velocity during Orbit 803 can be explained as the signature of plasma bubbles below but close to the satellite orbit. During Orbit 804, a series of ion density decreases (plasma bubbles) is detected over the shaded region, and the upward ion drift velocity within the reduced density regions is 200–400 m s^{-1}. The ion density decreases become deeper and wider, and the upward ion drift velocity becomes larger during Orbit 805. The structures of the ion density become relatively smooth during Orbit 806, and the upward ion drift velocity is still as high as 200 m s^{-1}. The longitudinal coverage of the plasma depletion region is ~35° (3800 km), and the ion density is reduced by 2–3 orders of magnitude.

[9] The enhanced upward ion velocity is first detected at the altitude of ~400 km during Orbit 803 If the upward ion drift is caused by the Rayleigh-Taylor instability, the Rayleigh-Taylor instability must have been excited at lower altitudes at an earlier time. The upward ion drift velocity is continuously growing from Orbit 803 to 805. The observations show that the growth time of the broad plasma depletions is longer than 3.3 h (two complete orbits). The upward ion drift is still significant when the depletion region approaches dawn during Orbit 806, implying that the plasma bubbles within the depletion region are still rising and do not become dead bubbles. *Huang et al.* [2011] found that the

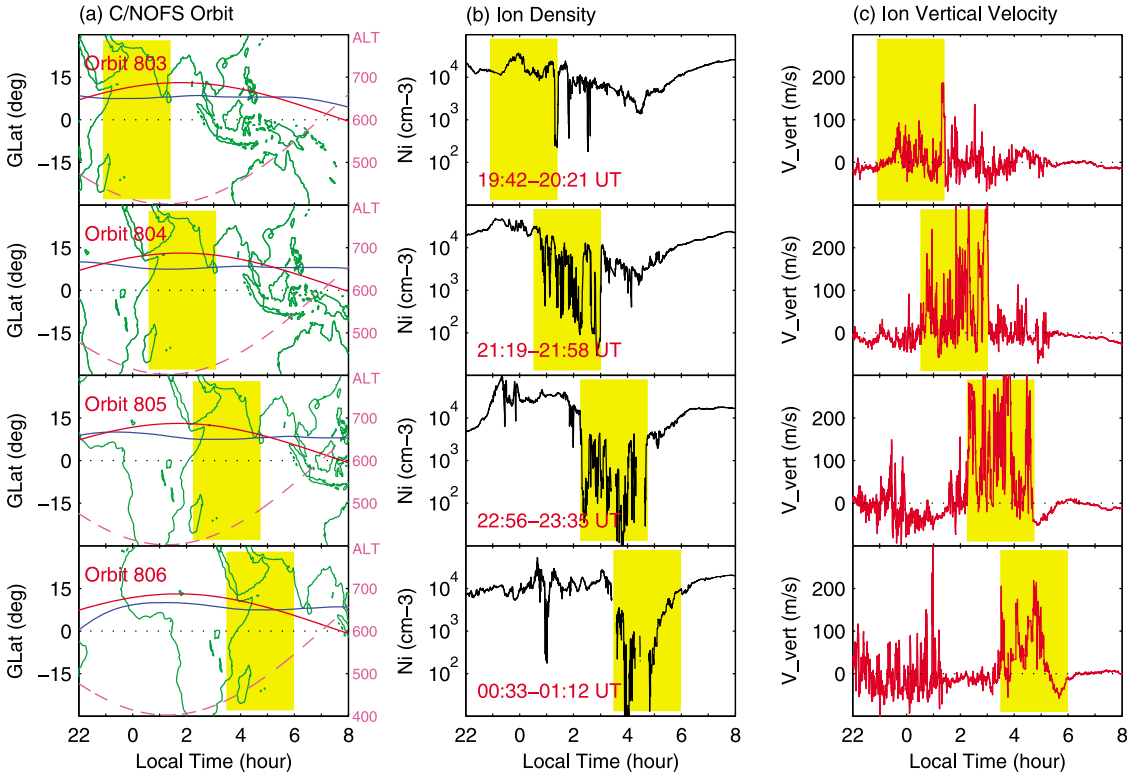

Figure 1. Low-latitude ionospheric ion density and ion vertical velocity measured by the C/NOFS satellite between 19:42 UT on 9 June 2008 and 01:12 UT on 10 June 2008. (a) The green lines depict the continents, the blue line depicts the magnetic equator, the solid red line represents the latitude of C/NOFS, and the dashed magenta line represents the altitude (in km) of C/NOFS labeled on the right. (b) The ion density and (c) ion vertical velocity. The yellow shading denotes the region of broad plasma depletions.

growth time of equatorial plasma bubbles is longer than 3.3 h and that the lifetime of the bubbles is longer than 7 h. The broad plasma depletions presented in Figure 1 are consistent with the long-lasting plasma bubbles reported by *Huang et al.* [2011].

[10] The large upward ion drift occurs only inside the density depletion region. In contrast, the ion vertical velocity in Figure 1c is generally downward outside the depletion region, and the downward plasma drift is consistent with the average pattern of the nighttime plasma drift in the equatorial ionosphere [*Fejer et al.*, 2008]. The upward plasma drift inside the shaded region and the downward plasma drift outside this region further justify that the enhanced upward plasma drift is related to the density decrease but not to the ambient plasma. The variations of the ion density become smooth between 05:00 and 06:00 LT during Orbit 806 because newly produced plasma particles by photoionization fill the depletion region, and the downward ion drift in this local time range is dominated by the average pattern of ionospheric plasma drift.

[11] The longitudinal range of the depletion region is nearly unchanged from Orbit 804 to 805. The depletion region during Orbit 806 has moved slightly to the west, compared to the previous orbits. The westward shift of the depletion region may be related to two processes. One process is the zonal drift of plasma bubbles [e.g., see *Huang et al.*, 2010, and references therein]. In general, plasma bubbles drift eastward in the evening and midnight sectors but westward near dawn. The westward drift of plasma bubbles could contribute to the shift of the depletion region between Orbit 805 and 806. Another possible process is that new plasma bubbles grow near the western boundary of the depletion region and merge with the existing depletions, resulting in the broadening of the depletion region in the westward direction.

[12] It can be seen in Figure 1 that small-scale structures exist in the ion density and vertical velocity in the depletion region. In order to depict the details of the structures, we plot the ion density and velocity data as a function of longitude for Orbits 804 and 805 in Figure 2. The data have a temporal resolution of 1 s, corresponding to a spatial resolution of ~7 km. Figures 2a and 2b clearly show the existence of a series of small-scale ion density decreases and corresponding ion velocity enhancements. The width of most individual ion velocity enhancements is ~1° in longitude (~100 km), and smaller-scale structures also exist. Figure 2c shows the horizontal component of the ion drift velocity. The ion zonal velocity is generally westward inside the depletion region but eastward outside the depletion region. The average zonal plasma drift in the equatorial ionosphere is eastward at night (between 17:00 and 06:00 LT) [*Fejer et al.*, 1991; *Pfaff et al.*, 2010]. In contrast, the plasma zonal drift inside equatorial plasma bubbles is determined by polarization electric field and is different from the zonal drift of the bubble structure [*Aggson et al.*, 1992; *Laakso et al.*, 1997; *Huang et al.*, 2010]. The westward ion drift inside the

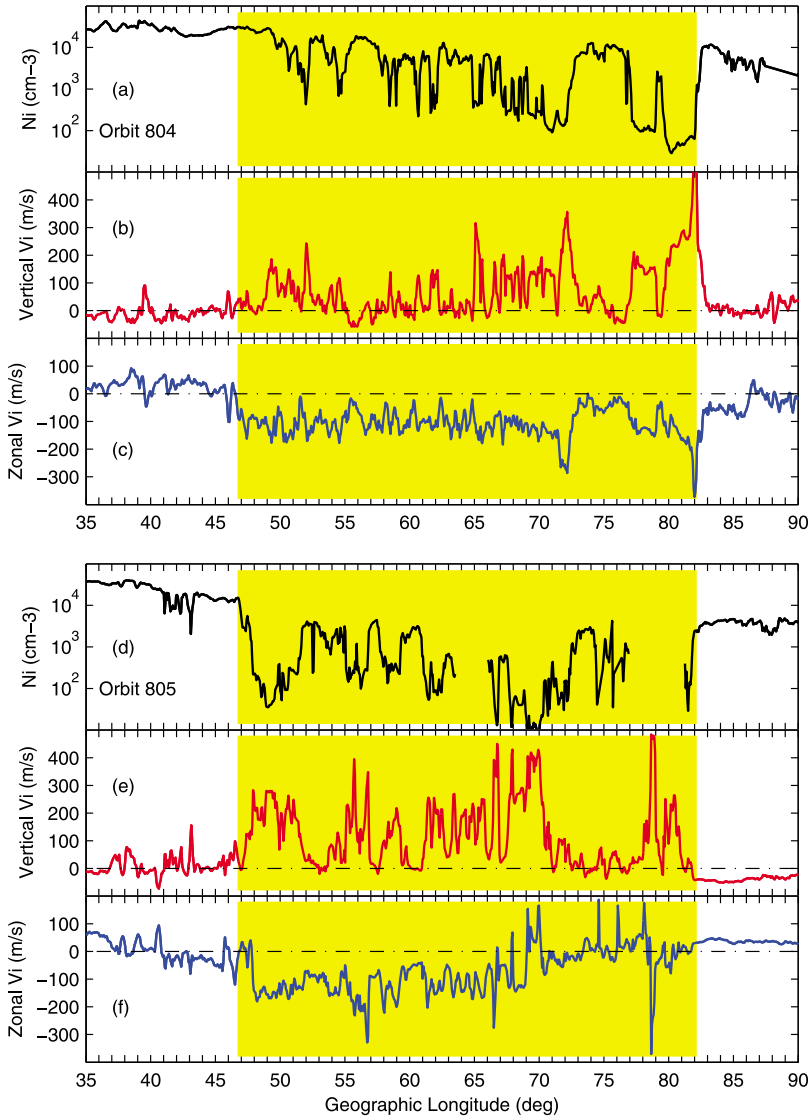

Figure 2. Longitudinal variations of the ion density and velocity during C/NOFS Orbits 804 and 805 on 9 June 2008. The zonal ion velocity is positive in the eastward direction. The yellow shading denotes the region of broad plasma depletions.

depletion region in our case suggests that the small-scale structures are related to equatorial plasma bubbles. During Orbit 805 (Figures 2d–2f), structures at scale length of ~100 km still exist in the ion density and vertical velocity, but wider regions of ion density depletions and velocity enhancements (3–5° in longitude) have occurred. It appears that some small-scale structures (~100 km in longitude) have merged to form the wider plasma depletions. During Orbit 806 (the bottom row of Figure 1), most plasma structures have disappeared, and a broad depletion region occurs. This is an excellent example that shows the evolution of multiple plasma bubbles into broad plasma depletions.

[13] The zonal drift of plasma bubbles may have important implication on the formation of broad plasma depletions. The drift velocity of plasma bubbles (the drift velocity of the bubble structure but not the drift velocity of plasma particles inside the bubble) is primarily determined by the drift of the ambient plasma, which is because bubbles are embedded in the ambient plasma. Jicamarca radar measurements show that the average zonal drift of the equatorial ionospheric *F* region plasma is eastward at night [*Fejer et al.*, 1991, 2005]. The eastward drift velocity of the *F* region plasma has a maximum value at ~20:00 LT, then gradually decreases, and becomes nearly zero near dawn. The zonal drift velocity of plasma bubbles and its variation with local time are similar to those of the average *F* region plasma drift [*Valladares et al.*, 1996; *Immel et al.*, 2003; *Park et al.*, 2007]. If a series of plasma bubbles exists and drifts eastward with the pattern of the average *F*-region plasma drift, the drift velocity of a bubble in the western (trailing) side is always faster than that of the bubble in the eastern (leading) side. When the bubbles approach a region where the drift velocity changes from eastward to westward, the first bubble at the eastern end of the bubble chain will first stop drifting eastward and start to drift westward, while the next bubble is still moving eastward. As a result, the two bubbles will become closer and

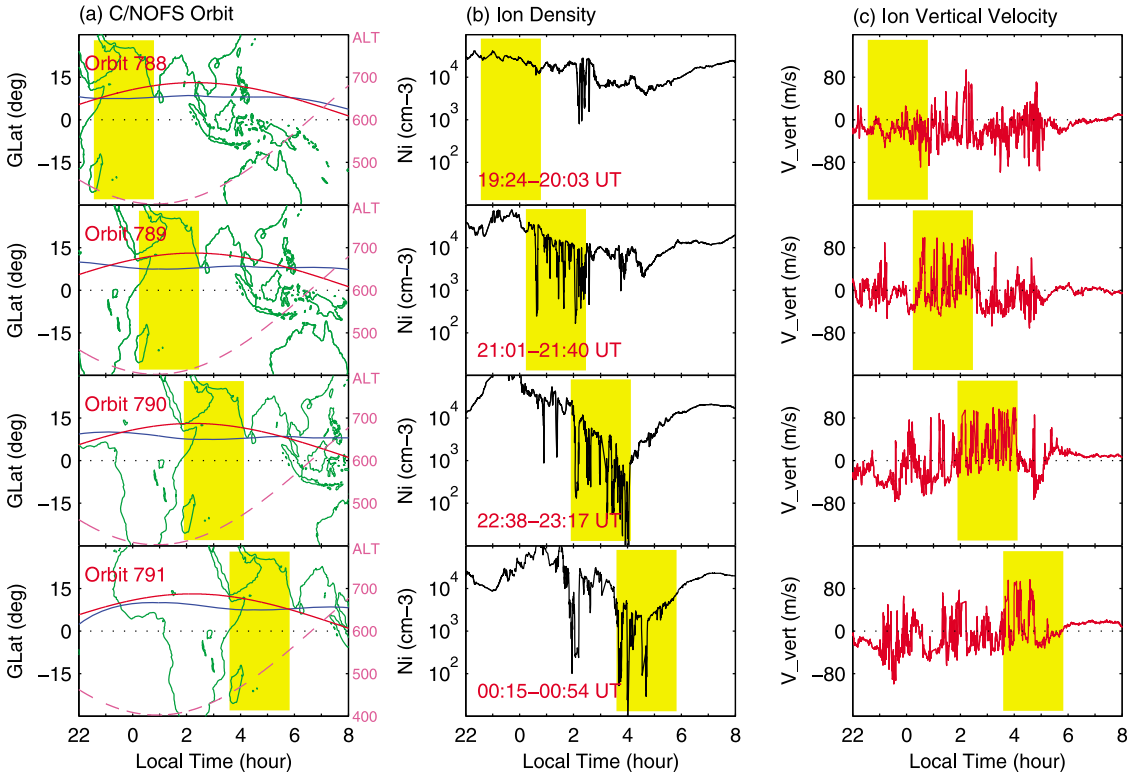

Figure 3. Same as Figure 1 but for the period from 19:24 UT on 8 June 2008 to 00:54 UT on 9 June 2008.

closer and finally collide (or merge) to form a new bubble. This process will continue until the last bubble at the western end of the bubble chain joins other bubbles. Because the merging process of plasma bubbles occurs most likely in the region of zonal drift reversal near dawn, broad plasma depletions form there.

[14] We present another example of broad plasma depletions in Figure 3. This case occurred on 8–9 June 2008. The ion density and vertical velocity do not show significant perturbations in the shaded region during Orbit 788. A series of ion density decreases and ion velocity enhancements with scale length of ~100 km in longitude is detected by C/NOFS during Orbit 789, and these density decreases with enhanced upward ion drift are plasma bubbles. During Orbit 790, the region of plasma bubbles has rotated to the local time range of 01:55–04:05. The plasma density decrease near the eastern edge of the shaded region over 03:40–04:05 LT appears to be a wide bubble with fine structures. Plasma bubbles also exist in other portions of the shaded region. The shaded region with multiple plasma bubbles approaches dawn during Orbit 791, and the ion density within this region is greatly decreased. In the local time range of 05:00–06:00, photoionization and atmospheric dynamic process become significant, the variation of the ion density becomes smooth, and the ion vertical velocity becomes downward. The longitudinal coverage of the broad depletions is ~30° (3300 km). The overall features of the broad plasma depletions in the case of Figure 3 are very similar to those in Figure 1.

[15] Figure 4 shows a case with three plasma bubbles. During Orbit 970, the ion density shows only a slight decrease in the shaded region. The altitude of C/NOFS is ~600 km in the shaded region, and plasma bubbles may exist at lower altitudes and have not reached the C/NOFS altitude. During Orbit 971, the altitude of C/NOFS is ~500 km in the shaded region, and three plasma bubbles are detected over a longitudinal range of ~800 km. Plasma bubbles are also detected at the same longitudes during Orbit 972. The ion velocity data are not plotted because of the data gap in the bubble region. The ion density is plotted as a function of geographic longitude in Figure 4c. Three separate bubbles can be clearly identified during Orbit 971. In contrast, the plasma depletion in the shaded region almost becomes a single, wider bubble during Orbit 972, although smaller-scale structures exist inside the depletion region. The plasma bubbles during the two successive orbits are located in the same longitudes. It is very likely the bubble during Orbit 972 is the same set of bubbles during Orbit 971. In other words, the three separate plasma bubbles during Orbit 971 have merged to form the single bubble during Orbit 972.

3. Numerical Simulations

[16] *Huang et al.* [2011] proposed that merging of multiple regular equatorial plasma bubbles results in the formation of broad plasma depletions. In order to explore whether the merging process can indeed occur, we use the physics-based ionospheric model (PBMOD) to simulate the evolution of plasma bubbles. This model was developed by *Retterer* [2005] to support the C/NOFS mission analysis and to forecast equatorial ionospheric structures and radio scintillations. The observed broad plasma depletions cover a

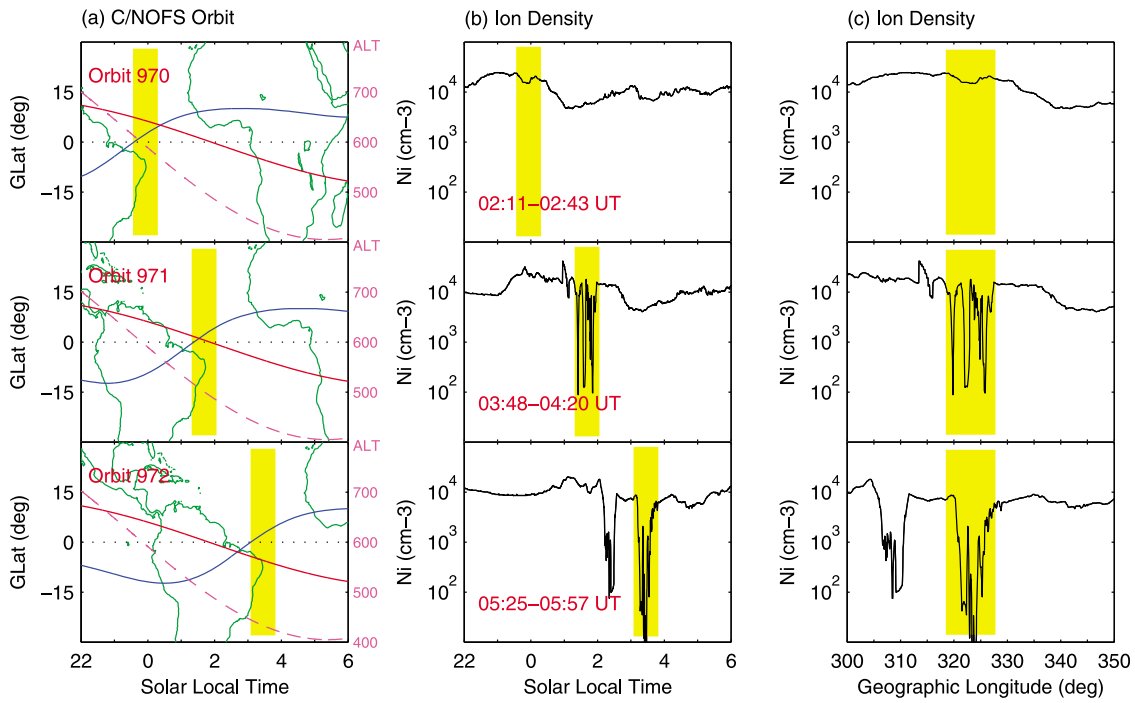

Figure 4. Low-latitude ionospheric ion density measured by the C/NOFS satellite between 02:11 and 05:57 UT on 21 June 2008. (a) The C/NOFS orbit. (b) The ion density as a function of local time and (c) as a function of longitude. The yellow shading denotes the region of plasma bubbles.

longitudinal range of 3300–3800 km. However, because of the limited computing capability, we cannot simulate the bubble phenomenon over such a large range. The Rayleigh-Taylor instability is excited in the bottomside *F* region with the largest gradient in the plasma density over an altitude range of ~100 km or so. In most numerical simulations, a fully developed plasma bubble caused by the Rayleigh-Taylor instability has a width of ~50 km in longitude [*Huba et al.*, 2009; *Retterer*, 2010a]. We use PBMOD to simulate the evolution of two plasma bubbles within a relatively small longitudinal range.

[17] The background ionosphere for the simulation is not specifically for deep solar minimum. In fact, the simulations were performed for multiple purposes with typical ionospheric parameters under solar max conditions. The simulations start when zero zonal distance is located at 18:00 LT. An initial perturbation with wavelength of 600 km and amplitude of 5% is imposed to the background plasma density. Figure 5 presents the evolution of the electron density in the equatorial ionosphere between 19:58 and 20:46 LT. The large-scale structure with wavelength of 600 km is caused by the initial perturbation, and the smaller-scale structures are generated spontaneously. It is obvious that plasma bubbles grow from the wave peak region where the bottomside *F* region has been moved to higher altitudes. Figure 6 presents the corresponding structures in the vertical ion velocity.

[18] Two plasma bubbles become clear between −500 and −400 km at 20:10 LT. The major bubble on the right reaches ~600 km altitude at 20:16 LT. At 20:22 LT, the upper portion of the major bubble tilts to the west, and the lower portion is nearly upright. In contrast, the minor bubble on the left tilts to the east. The upper portion of the two bubbles has merged in the altitude range of 500–560 km at 20:22 LT, which can be more easily seen in the velocity plots (Figure 6). At 20:28 LT, the bottom portion of the two bubbles has also merged, and only in the altitude range of 400–460 km are the two bubbles still separated. The separated portion of the two bubbles becomes very small at 20:34 LT and completely disappears at 20:40 LT. The two bubbles have merged to form a single bubble.

[19] Figure 6 shows the ion vertical velocity during the merging process of the two plasma bubbles. The ion velocity is upward inside the two bubbles and downward between (and outside) the bubbles. At 20:22 LT, the ion velocity is upward within the merged portion of the two bubbles in the altitude range of 500–560 km and downward in the separated portion of two bubbles between 400 and 500 km. The high density region with downward plasma flow completely disappears at 20:40 LT, and the ion velocity is upward everywhere inside the merged, single bubble.

4. Discussion

[20] The occurrence of spread F irregularities in the low-latitude ionosphere shows unusual features during solar minimum. *Patra et al.* [2009] found that F region field-aligned irregularities detected by a mesosphere-stratosphere-troposphere radar at 6.4°N magnetic latitude during the summer of low solar condition were mostly confined to the postmidnight hours. *Candido et al.* [2011] analyzed the spread F events over a location under the southern crest of the equatorial ionization anomaly during the last solar cycle and verified high spread F occurrence around midnight-postmidnight during June solstice when the solar flux reached very low values. They found that the spread F onset

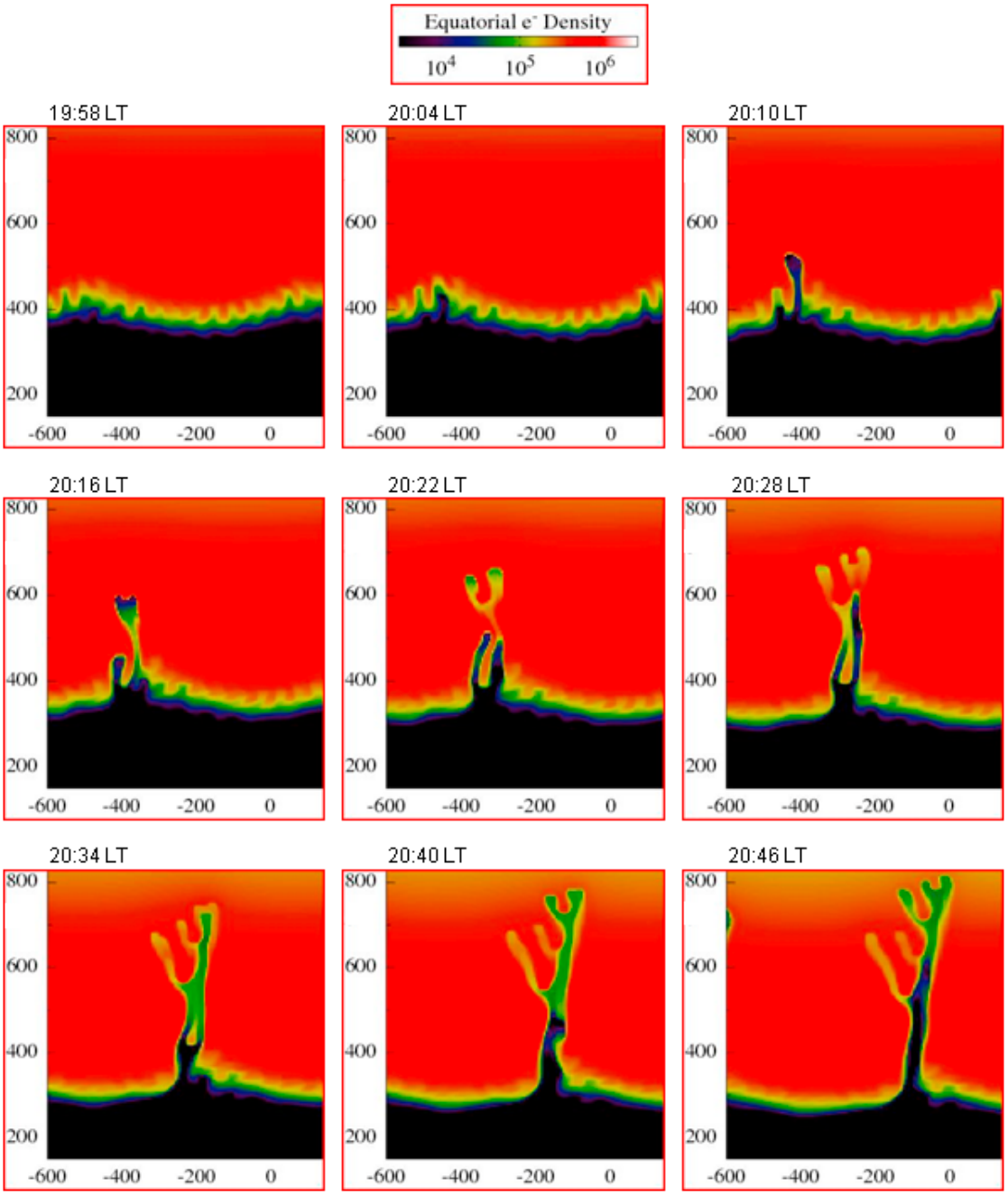

Figure 5. Numerical simulations of the evolution of equatorial plasma bubbles during merging process: Electron density. The horizontal axis is zonal (west-east) distance in km, and the vertical axis is altitude in km.

times are distributed at later evening hours with the peak being at ~23:00 LT. *Sobral et al.* [2011] studied the midnight reversal of the zonal drift velocity of ionospheric plasma bubble during geomagnetically quiet times, and the dominant forcing mechanism for westward drifting bubbles was identified to be the westward thermospheric wind. The occurrence of spread F is related to the *F* region plasma distribution. The F-peak electron density and total electron content are lower during solar minimum than those during solar maximum [*Araujo-Pradere et al.*, 2011; *Liu et al.*, 2011].

[21] In this paper, we focus on the broad plasma depletions detected by the C/NOFS satellite near dawn. The observations presented in Figures 1–3 show that a series of ion density decreases and ion velocity enhancements is first detected near midnight over a longitudinal range of 30–35°. Each individual ion density decrease covers ~100 km in longitude, and the density is reduced by 1–3 orders of magnitude. The scale length of an individual ion density decrease is comparable to the width of a fully developed plasma bubble [*Tsunoda*, 1983; *Huba et al.*, 2009; *Retterer*, 2010a]. The ion velocity is upward and reaches 200–400 m s^{-1} inside

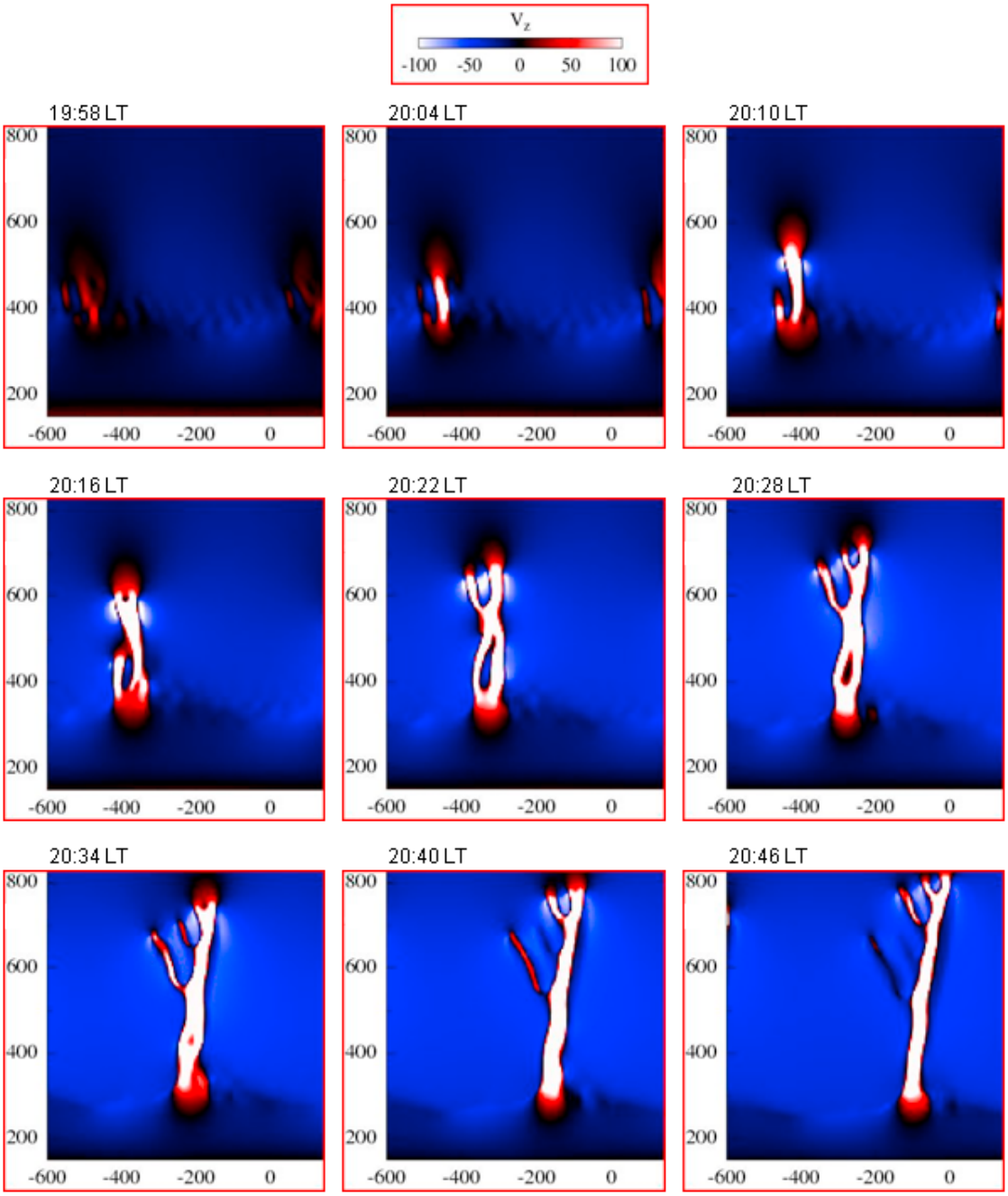

Figure 6. Numerical simulations of the evolution of equatorial plasma bubbles during merging process: Ion vertical velocity.

the region of the density decreases, and the large upward ion drift is a typical feature of plasma bubbles caused by the Rayleigh-Taylor instability. Therefore the ion density decreases with large upward ion drift are identified as equatorial plasma bubbles. The westward drift of plasma particles in the reduced density regions in Figure 2c provides further evidence for the occurrence of plasma bubbles. The longitudinal scale length of the plasma bubbles becomes larger (the third row of Figures 1 and 3), suggesting that some bubbles have combined to form wider bubbles. When they rotate to the dawn sector (04:00–06:00 LT), the plasma bubbles actually have become typical broad plasma depletions (the fourth row in Figures 1 and 3). *Huang et al.* [2011] proposed that broad plasma depletions result from merging of multiple plasma bubbles. The observations presented in this paper provide new evidence that supports the merging scenario.

[22] In the case reported by *Huang et al.* [2011], the longitudinal coverage of the plasma depletions is ~20° (2200 km). Smaller-scale structures are obvious in the ion velocity data. Because C/NOFS is located at 10–15° magnetic latitudes in their case, plasma density decreases at smaller scale are not clear. In the cases presented in this paper, the orbit of C/NOFS is close to the magnetic equator,

and the plasma density decreases and corresponding upward ion drift with a characteristic scale length of ~100 km in longitude can be clearly identified. The longitudinal coverage of the plasma bubbles and resultant broad depletions is as large as 3300–3800 km.

[23] The observations in Figures 1–3 present a very unusual phenomenon in the nightside equatorial ionosphere. A radar detects plasma bubbles at a fixed longitude, and satellites with large inclination angles fly across the equatorial ionosphere only over a limited longitude range. In contrast, the C/NOFS satellite, with unique design of its orbit, can fly along, or very close to, the magnetic equator over several thousands of kilometers and is able to detect plasma bubbles, if they exist, over a large longitudinal range. This longitudinal range is not the extension of a depleted flux tube (a single bubble) along the magnetic field lines.

[24] The generation mechanism of the broad plasma depletions has not been fully understood. *Huang et al.* [2011] suggested that multiple bubbles merge to form the broad depletions. The observations and simulations presented in this paper are consistent with the merging mechanism. However, an important issue is how the high-density barriers between plasma depletions (bubbles) can be removed in the ionospheric plasma. One might argue that the barriers would always exist because the plasma flow is incompressible. However, the removal of the barriers can occur without requirement of compression. In the numerical simulations presented in Figures 5 and 6, the two bubbles are first merged in the altitude range of 500–560 km at 20:22 LT, resulting in the formation of a downward moving, high-density island in the altitude range of 400–500 km. The high-density island with downward velocity becomes smaller at 20:28 LT and almost disappears at 20:34 LT. Comparing the ion velocity plots at 20:22 and 20:28 UT, the location of the upper boundary of the high-density region has moved downward over the period of 6 min, while the location of the lower boundary is almost unchanged.

[25] We propose the following scenario to explain the disappearance of the high-density region. The plasma flow is downward in the high-density region. When the high-density region moves downward, no plasma particles will fill this region from above because the merged portion above is almost empty. Therefore the location of the upper boundary of the high-density region continuously moves to lower altitudes. However, the polarization electric field in the bottom portion of the bubble, just beneath the high density region, is eastward and drives upward $\mathbf{E} \times \mathbf{B}$ drift, so the downward moving dense plasma cannot enter the bottom portion of the bubbles. Instead, the dense plasma will flow toward higher-latitudes (lower altitudes at off-equatorial locations) along the geomagnetic field lines and be neutralized through recombination. The high-density region will finally disappear when all plasma particles have flown to higher latitudes and been recombined there. The numerical simulations demonstrate for the first time that the merging process of multiple bubbles can indeed occur in the incompressible ionospheric plasma.

[26] It should be mentioned that the simulation results cannot be directly compared with the observations. The broad plasma depletions detected by C/NOFS have a longitudinal coverage of 3300–3800 km. In contrast, the longitudinal width of the merged bubble in the simulations is ~100 km. The simulations verify that two plasma bubbles can merge to form a wider bubble and that the merging mechanism is valid. However, the model has not been able to reproduce the occurrence of a series of plasma bubbles over a longitude range of thousands of kilometers and the formation of broad plasma depletions through merging. As we mentioned in the previous section, the simulations were performed under solar maximum conditions. The broad plasma depletions are observed during deep solar minimum and perhaps determined by the ionospheric and thermospheric conditions under extremely low solar activity.

[27] The ionospheric and atmospheric conditions are remarkably different between solar maximum and solar minimum periods. Both the vertical plasma drift at prereversal enhancement and the nighttime eastward plasma drift in the equatorial ionosphere during solar maximum are much higher than those during solar minimum [*Fejer et al.*, 1991, 2005]. The *F* region plasma density is high during solar maximum and low during solar minimum [*Kelley*, 1989]. The dense plasma barrier between successive bubbles and the ratio of the plasma density inside the bubbles to the high-density barrier vary with the solar conditions. The growth rate of the Rayleigh-Taylor instability depends on the altitude distribution of plasma density, as well as on the ion-neutral collision frequency that is linearly proportional to the neutral density. The atmospheric neutral density at 400-km altitude during the last solar minimum years (2008–2009) is about 10 times smaller than that during solar maximum years [*Solomon et al.*, 2010]. These ionospheric and thermospheric parameters significantly influence the growth of equatorial plasma bubbles and the altitude range at which plasma bubbles start to merge. Therefore the merging processes of plasma bubbles under solar minimum conditions can be very different from those under solar maximum conditions. A good understanding of specific ionospheric-thermospheric parameters under solar minimum conditions is required to reproduce the broad plasma depletions by numerical models. We plan to simulate the merging process of plasma bubbles under solar minimum conditions in the future.

[28] We also want to indicate the limitation of the C/NOFS measurements in identifying the causal mechanism of broad plasma depletions. The orbital period of C/NOFS is ~100 min. We cannot determine how plasma bubbles evolve within the interval of 100 min from C/NOFS measurements alone. When plasma bubbles occur at the same longitudes during two successive orbits, they are assumed to be the same set of bubbles. For example, in Figure 4, the three separate bubbles during Orbit 971 and the single bubble during Orbit 972 exist at the same longitudes. It is unlikely that the three bubbles during Orbit 971 are completely extinguished and the single bubble during Orbit 972 is a newly generated one within 100 min. Instead the single bubble during Orbit 972 is explained to result from the merging of the three bubbles during the previous orbit. However, we do not have other measurements to verify that the three bubbles indeed evolve into the single bubble. We will find other instrument measurements to examine the evolution and merging process of plasma bubbles.

[29] Broad plasma depletions with distinct characteristics have been observed. In the observations presented by *Huang et al.* [2009], the vertical ion drift inside the depletion region is small or weakly downward. In the cases reported by *de La*

Beaujardière et al. [2009] and *Su et al.* [2009], the variation of the ion density in the depletion region near dawn is relatively smooth. In contrast, *Huang et al.* [2011] and this paper show that the ion density and velocity inside the depletion region are highly structured. These structures are related to plasma bubbles, and the ion flow is strongly upward. It has not been understood what determines the generation of different broad depletions and how these depletions are related to the solar, ionospheric, and atmospheric conditions. These issues require further investigations in the future.

5. Summary

[30] A spectacular phenomenon observed by the C/NOFS satellite in the equatorial ionosphere is the occurrence of plasma bubbles over several thousands of kilometers in longitude near dawn. A series of plasma bubbles is first detected around midnight. The plasma bubbles then rotate to the dawn sector and evolve into broad plasma depletions. The plasma flow inside the bubbles and resultant broad depletions is strongly upward (200–400 m s^{-1}) for 5 h, and the plasma bubbles are continuously moving upward when they reach the dawn sector. This is the first observation of the existence of equatorial plasma bubbles with strong upward plasma flow over 3800 km in longitude. The observation reveals that the equatorial ionosphere can be highly disturbed and become extremely turbulent during solar minimum.

[31] We have used the physics-based low-latitude ionospheric model to simulate the merging process of plasma bubbles. In the simulations, two plasma bubbles grow and connect first at the altitude range of 500–560 km. The high plasma density region between the two bubbles disappears within 10–20 min, and the two bubbles merge to form a single wider bubble. The interpretation of the disappearance of the high density region between the two bubbles is that the dense plasma moves along the geomagnetic field lines to lower altitudes (at higher latitudes) and is recombined there. The simulations show that the merging process of plasma bubbles can indeed occur in incompressible ionospheric plasma. The simulation results support the merging mechanism for the formation of broad plasma depletions.

[32] **Acknowledgments.** Work by C.S.H. was supported by the Air Force Office of Scientific Research (AFOSR) award FA9550-09-1-0321. The C/NOFS mission is supported by the Air Force Research Laboratory, the Department of Defense Space Test Program, the National Aeronautics and Space Administration (NASA), the Naval Research Laboratory, and the Aerospace Corporation.

[33] Robert Lysak thanks the reviewers for their assistance in evaluating this paper.

References

Aggson, T. L., N. C. Maynard, W. B. Hanson, and J. L. Saba (1992), Electric field observations of equatorial bubbles, *J. Geophys. Res.*, *97*(A3), 2997–3009, doi:10.1029/90JA02356.

Araujo-Pradere, E. A., R. Redmon, M. Fedrizzi, R. Viereck, and T. J. Fuller-Rowell (2011), Some characteristics of the ionospheric behavior during the solar cycle 23–24 minimum, *Sol. Phys.*, *274*, 439–456, doi:10.1007/s11207-011-9728-3.

Burke, W. J., O. de La Beaujardière, L. C. Gentile, D. E. Hunton, R. F. Pfaff, P. A. Roddy, Y.-J. Su, and G. R. Wilson (2009), C/NOFS observations of plasma density and electric field irregularities at post-midnight local times, *Geophys. Res. Lett.*, *36*, L00C09, doi:10.1029/2009GL038879.

Candido, C. M. N., I. S. Batista, F. Becker-Guedes, M. A. Abdu, J. H. A. Sobral, and H. Takahashi (2011), Spread F occurrence over a southern anomaly crest location in Brazil during June solstice of solar minimum activity, *J. Geophys. Res.*, *116*, A06316, doi:10.1029/2010JA016374.

de La Beaujardière, O., et al. (2009), C/NOFS observations of deep plasma depletions at dawn, *Geophys. Res. Lett.*, *36*, L00C06, doi:10.1029/2009GL038884.

Fejer, B. G., E. R. de Paula, S. A. González, and R. F. Woodman (1991), Average vertical and zonal F region plasma drifts over Jicamarca, *J. Geophys. Res.*, *96*(A8), 13,901–13,906, doi:10.1029/91JA01171.

Fejer, B. G., J. R. Souza, A. S. Santos, and A. E. Costa Pereira (2005), Climatology of F region zonal plasma drifts over Jicamarca, *J. Geophys. Res.*, *110*, A12310, doi:10.1029/2005JA011324.

Fejer, B. G., J. W. Jensen, and S.-Y. Su (2008), Quiet time equatorial *F* region vertical plasma drift model derived from ROCSAT-1 observations, *J. Geophys. Res.*, *113*, A05304, doi:10.1029/2007JA012801.

Haerendel, G. (1973), Theory of equatorial spread-F, technical report, Max Planck Inst. fur Extraterr. Phys., Munich, Germany.

Huang, C.-S., and M. Kelley (1996a), Nonlinear evolution of equatorial spread F: 1. On the role of plasma instabilities and spatial resonance associated with gravity wave seeding, *J. Geophys. Res.*, *101*(A1), 283–292, doi:10.1029/95JA02211.

Huang, C.-S., and M. Kelley (1996b), Nonlinear evolution of equatorial spread F: 2. Gravity wave seeding of Rayleigh-Taylor instability, *J. Geophys. Res.*, *101*(A1), 293–302, doi:10.1029/95JA02210.

Huang, C.-S., O. de La Beaujardiere, R. F. Pfaff, J. M. Retterer, P. A. Roddy, D. E. Hunton, Y.-J. Su, S.-Y. Su, and F. J. Rich (2010), Zonal drift of plasma particles inside equatorial plasma bubbles and its relation to the zonal drift of the bubble structure, *J. Geophys. Res.*, *115*, A07316, doi:10.1029/2010JA015324.

Huang, C.-S., O. de La Beaujardiere, P. A. Roddy, D. E. Hunton, R. F. Pfaff, C. E. Valladares, and J. O. Ballenthin (2011), Evolution of equatorial ionospheric plasma bubbles and formation of broad plasma depletions measured by the C/NOFS satellite during deep solar minimum, *J. Geophys. Res.*, *116*, A03309, doi:10.1029/2010JA015982.

Huang, C. Y., F. A. Marcos, P. A. Roddy, M. R. Hairston, W. R. Coley, C. Roth, S. Bruinsma, and D. E. Hunton (2009), Broad plasma decreases in the equatorial ionosphere, *Geophys. Res. Lett.*, *36*, L00C04, doi:10.1029/2009GL039423.

Huba, J. D., J. Krall, and G. Joyce (2009), Atomic and molecular ion dynamics during equatorial spread F, *Geophys. Res. Lett.*, *36*, L10106, doi:10.1029/2009GL037675.

Immel, T. J., S. B. Mende, H. U. Frey, L. M. Peticolas, and E. Sagawa (2003), Determination of low latitude plasma drift speeds from FUV images, *Geophys. Res. Lett.*, *30*(18), 1945, doi:10.1029/2003GL017573.

Kelley, M. C. (1989), *The Earth's Ionosphere: Plasma Physics and Electrodynamics*, Academic Press, San Diego, Calif.

Kelley, M. C., et al. (1986), The Condor equatorial spread F campaign: Overview and results of the large-scale measurements, *J. Geophys. Res.*, *91*(A5), 5487–5503, doi:10.1029/JA091iA05p05487.

Kelley, M. C., F. S. Rodrigues, J. J. Makela, R. Tsunoda, P. A. Roddy, D. E. Hunton, J. M. Retterer, O. de La Beaujardiere, E. R. de Paula, and R. R. Ilma (2009), C/NOFS and radar observations during a convective ionospheric storm event over South America, *Geophys. Res. Lett.*, *36*, L00C07, doi:10.1029/2009GL039378.

Keskinen, M. J., S. L. Ossakow, and B. G. Fejer (2003), Three-dimensional nonlinear evolution of equatorial ionospheric spread-*F* bubbles, *Geophys. Res. Lett.*, *30*(16), 1855, doi:10.1029/2003GL017418.

Krall, J., J. D. Huba, S. L. Ossakow, and G. Joyce (2010), Why do equatorial ionospheric bubbles stop rising?, *Geophys. Res. Lett.*, *37*, L09105, doi:10.1029/2010GL043128.

Laakso, H., N. C. Maynard, R. F. Pfaff, T. L. Aggson, W. R. Coley, P. Janhunen, and F. A. Herrero (1997), Electric field diagnostics of the dynamics of equatorial density depletions, *J. Atmos. Sol. Terr. Phys.*, *59*(13), 1625–1631, doi:10.1016/S1364-6826(96)00161-7.

Liu, L., Y. Chen, H. Le, V. I. Kurkin, N. M. Polekh, and C.-C. Lee (2011), The ionosphere under extremely prolonged low solar activity, *J. Geophys. Res.*, *116*, A04320, doi:10.1029/2010JA016296.

Park, S. H., S. L. England, T. J. Immel, H. U. Frey, and S. B. Mende (2007), A method for determining the drift velocity of plasma depletions in the equatorial ionosphere using far-ultraviolet spacecraft observations, *J. Geophys. Res.*, *112*, A11314, doi:10.1029/2007JA012327.

Patra, A. K., D. V. Phanikumar, and T. K. Pant (2009), Gadanki radar observations of *F* region field-aligned irregularities during June solstice of solar minimum: First results and preliminary analysis, *J. Geophys. Res.*, *114*, A12305, doi:10.1029/2009JA014437.

Pfaff, R., et al. (2010), Observations of DC electric fields in the low-latitude ionosphere and their variations with local time, longitude, and plasma density during extreme solar minimum, *J. Geophys. Res.*, *115*, A12324, doi:10.1029/2010JA016023.

Retterer, J. M. (2005), Physics-based forecasts of equatorial radio scintillation for the Communication and Navigation Outage Forecasting System (C/NOFS), *Space Weather*, *3*, S12C03, doi:10.1029/2005SW000146.

Retterer, J. M. (2010a), Forecasting low-latitude radio scintillation with 3-D ionospheric plume models: 1. Plume model, *J. Geophys. Res.*, *115*, A03306, doi:10.1029/2008JA013839.

Retterer, J. M. (2010b), Forecasting low-latitude radio scintillation with 3-D ionospheric plume models: 2. Scintillation calculation, *J. Geophys. Res.*, *115*, A03307, doi:10.1029/2008JA013840.

Scannapieco, A. J., and S. L. Ossakow (1976), Nonlinear spread-*F*, *Geophys. Res. Lett.*, *3*(8), 451–454, doi:10.1029/GL003i008p00451.

Sobral, J. H. A., et al. (2011), Midnight reversal of ionospheric plasma bubble eastward velocity to westward velocity during geomagnetically quiettime: Climatology and its model validation, *J. Atmos. Sol. Terr. Phys.*, *73*(11–12), 1520–1528, doi:10.1016/j.jastp.2010.11.031.

Solomon, S. C., T. N. Woods, L. V. Didkovsky, J. T. Emmert, and L. Qian (2010), Anomalously low solar extreme-ultraviolet irradiance and thermospheric density during solar minimum, *Geophys. Res. Lett.*, *37*, L16103, doi:10.1029/2010GL044468.

Su, Y.-J., J. M. Retterer, O. de La Beaujardière, W. J. Burke, P. A. Roddy, R. F. Pfaff, G. R. Wilson, and D. E. Hunton (2009), Assimilative modeling of equatorial plasma depletions observed by C/NOFS, *Geophys. Res. Lett.*, *36*, L00C02, doi:10.1029/2009GL038946.

Su, Y.-J., J. M. Retterer, R. F. Pfaff, P. A. Roddy, O. de La Beaujardière, and J. O. Ballenthin (2011), Assimilative modeling of observed postmidnight equatorial plasma depletions in June 2008, *J. Geophys. Res.*, *116*, A09318, doi:10.1029/2011JA016772.

Tsunoda, R. T. (1983), On the generation and growth of equatorial backscatter plumes: 2. Structuring of the west walls of upwellings, *J. Geophys. Res.*, *88*(A6), 4869–4874, doi:10.1029/JA088iA06p04869.

Tsunoda, R. T., and B. R. White (1981), On the generation and growth of equatorial backscatter plumes: 1. Wave structure in the bottomside *F* layer, *J. Geophys. Res.*, *86*(A5), 3610–3616, doi:10.1029/JA086iA05p03610.

Valladares, C., R. Sheehan, S. Basu, H. Kuenzler, and J. Espinoza (1996), The multi-instrumented studies of equatorial thermosphere aeronomy scintillation system: Climatology of zonal drifts, *J. Geophys. Res.*, *101*(A12), 26,839–26,850, doi:10.1029/96JA00183.

Woodman, R., and C. La Hoz (1976), Radar observations of *F* region equatorial irregularities, *J. Geophys. Res.*, *81*(31), 5447–5466, doi:10.1029/JA081i031p05447.

Zalesak, S., S. Ossakow, and P. Chaturvedi (1982), Nonlinear equatorial spread F: The effect of neutral winds and background Pedersen conductivity, *J. Geophys. Res.*, *87*(A1), 151–166, doi:10.1029/JA087iA01p00151.

J. O. Ballenthin, O. de La Beaujardiere, C.-S. Huang, D. E. Hunton, and P. A. Roddy, Space Vehicles Directorate, Air Force Research Laboratory, 3550 Aberdeen Ave. SE, Kirtland AFB, NM 87117, USA. (chaosong.huang@kirtland.af.mil)

R. F. Pfaff, Space Weather Laboratory, NASA Goddard Space Flight Center, Mail Code 674, Greenbelt, MD 20771, USA.

J. M. Retterer, Institute for Scientific Research, Boston College, 149 Commonwealth Ave., Chestnut Hill, MA 02467, USA.